applied sciences

MDPI

Article

Comparative Performance Analysis of Small Concrete Beams Reinforced with Steel Bars and Non-Metallic Reinforcements

Abel A. Belay, Julita Krassowska * and Marta Kosior-Kazberuk

Department of Building Structures and Structural Mechanics, Bialystok University of Technology, Wiejska 45A, 15-351 Bialystok, Poland; abel.belay@sd.pb.edu.pl (A.A.B.); m.kosior@pb.edu.pl (M.K.-K.)
* Correspondence: j.krassowska@pb.edu.pl

Abstract: This research investigates the performance of small concrete beams that are reinforced with glass fiber-reinforced polymer (GFRP) bars, basalt fiber-reinforced polymer (BFRP) bars, and traditional steel bars. It addresses the limitations of traditional steel reinforcement, emphasizing the need for alternative strategies. Fiber-reinforced polymer (FRP) materials, including GFRP and BFRP, are examined for their mechanical characteristics compared to steel. The experimental program focuses on ultimate load-bearing capacity, deflection, deformation at different load levels, and failure modes. The concrete specimens, prepared according to Eurocode, consist of six small concrete beams measuring 80 × 120 × 1100 mm with varied reinforcements. The study reveals that GFRP-reinforced beams outperform BFRP and steel reinforcements in ultimate load-bearing capacity, showcasing enhanced structural performance. The GFRP-reinforced beams exhibit capacity and resilience characteristics surpassing those of both BFRP and steel, whereas the deflection observed was higher on both fiber-reinforced beams than on the steel-reinforced beams. The examination of failure modes reveals that the concrete beams that were reinforced with FRP bars showed a bending property before failure, while those reinforced with steel broke easily without bending much. This comprehensive research contributes to advancing our understanding of FRP materials' application in concrete structures, paving the way for further optimization and overcoming limitations in reinforcement materials.

Keywords: BFRP bars; GFRP bars; concrete beam; steel bars

check for updates

Citation: Belay, A.A.; Krassowska, J.; Kosior-Kazberuk, M. Comparative Performance Analysis of Small Concrete Beams Reinforced with Steel Bars and Non-Metallic Reinforcements. *Appl. Sci.* **2024**, *14*, 3957. https://doi.org/10.3390/app14103957

Academic Editor: José Manuel Moreno-Maroto

Received: 10 April 2024
Revised: 30 April 2024
Accepted: 1 May 2024
Published: 7 May 2024

1. Introduction

Concrete, a commonly used building material, is often deficient in tension strength and susceptible to fractures from shrinkage and plastic deformation [1]. This inherent weakness in tension makes plain concrete unsuitable for many structural applications, as even structures under compressive pressures require sufficient tensile strength to prevent buckling. Steel, renowned for its remarkable tensile strength, has been widely employed in the construction industry to reinforce structural components, making it an ideal material for enhancing the strength of concrete buildings. Despite its widespread use, steel reinforcement comes with drawbacks, as highlighted by Mahadev Desai [2]. Corrosion vulnerability is a significant concern, with steel rusting over time when exposed to oxygen and moisture, compromising its structural integrity. Environmental factors, such as high seawater quantities in coastal areas or elevated humidity, can expedite the corrosion process, leading to fractures and spalling in the adjacent concrete, thereby impacting the overall structural stability. Another drawback is the substantial weight of the steel reinforcement due to its density, which contributes significantly to the overall weight of the construction when used in large quantities [3,4].

The inherent limitations in traditional steel reinforcement methods within construction have spurred a thorough exploration of alternative approaches, driven by significant advancements in science and technology. In response to this imperative, there has been a surge of research interest surrounding the utilization of fiber reinforcements, with studies investigating the characteristics and tensile strengths of various fiber materials to augment their applicability in structural contexts [5,6].

Among the alternatives, fiber-reinforced polymer (FRP) materials have emerged as particularly promising contenders for different infrastructure projects. Their adoption is underpinned by a myriad of compelling advantages, including but not limited to rapid manufacturing and installation processes, inherent lightweight properties facilitating ease of handling, long-term cost-effectiveness due to reduced maintenance requirements, exceptional corrosion resistance, and an extended service life. Such attributes position FRP materials as versatile solutions that are amenable to a wide spectrum of applications across infrastructure construction domains [7–10].

In the realm of civil engineering, the utilization of four primary fiber materials—carbon, glass, aramid, and basalt—dominates the production of reinforced fibers. These fibers serve as the building blocks for the creation of distinct reinforced polymers, encompassing Carbon Fiber-Reinforced Polymer (CFRP), glass fiber-reinforced polymer (GFRP), Aramid Fiber-Reinforced Polymer (AFRP), and basalt fiber-reinforced polymer (BFRP). Each variant of reinforced polymer exhibits a unique array of properties, rendering them apt for specific applications within the civil engineering landscape [6,11–13]. This rich diversity in fiber reinforcement options underscores the nuanced and multifaceted nature of material selection processes within the realm of structural engineering.

Recently, numerous studies have explored the intricate properties of fiber-reinforced polymer (FRP)-reinforced concrete beams, as evidenced by a growing body of research [14–17]. Many of these investigations have focused on the behavior of concrete beams that are reinforced with a single type of fiber reinforcement, comparing their performance against that of conventional steel-reinforced concrete beams [16–22]. Conversely, other studies [23–29] have chosen to examine FRP bars in isolation, subjecting them to various conditions to elucidate their intrinsic properties without integration into concrete structures. While these studies offer valuable insights into the material properties of FRPs, there remains a notable gap in understanding how these materials function within the broader context of concrete elements. Additionally, a study comparing the adhesion properties of FRP fibers, coupled with analytical evaluations of material properties, was conducted [29]. However, the focus on standalone bar analysis overlooks the crucial aspect of comprehensively understanding the interaction between these materials and concrete elements, particularly in load-carrying scenarios.

Among the studies on the ultimate load-carrying capacity of concrete beams reinforced with FRP bars, Urbanski et al. [18] meticulously documented performance metrics, revealing that the average ultimate load of three concrete beams reinforced with 8 mm basalt fiber-reinforced polymer (BFRP) bars was 40 kN, while their steel-reinforced counterparts managed a load of 35 kN. This stark contrast signifies a notable 14.28% increase in the ultimate load-carrying capacity of BFRP-reinforced concrete beams compared to their steel-reinforced counterparts. The impressive tensile strength property inherent in FRP reinforcement is further underscored by the ACI Committee 440 [30].

Moreover, Sirimontree [22] conducted a parallel investigation, discovering that concrete beams reinforced with glass fiber-reinforced polymer (GFRP) bars exhibited an average ultimate load of 70.5 kN, nearly doubling that of steel-reinforced beams. Our research corroborates these findings, demonstrating that concrete beams reinforced with GFRP bars sustained an average ultimate load of 36.9 kN, while those reinforced with BFRP bars sustained 28.4 kN. These figures represent remarkable increases of 76.55% and 35.88%, respectively, compared to concrete beams reinforced with steel bars (20.9 kN).

Regarding the deflection property, some scholars [18,31] documented significantly greater deflections in beams reinforced with BFRP bars compared to reference beams. This phenomenon was attributed to the lower modulus of BFRP bars compared to steel bars. Furthermore, Kosior-Kazberuk et al. [16] reported that concrete beams reinforced with basalt fiber polymers exhibited substantially higher deformations, averaging three to four times more than steel-reinforced concrete beams. Notably, during the initial loading phase, BFRP-reinforced concrete beams demonstrated a 40% increase in deflection relative to reference reinforced concrete (RC) beams, with this disparity increasing as the load intensified. Consequently, BFRP-reinforced concrete beams exhibited deflections twice as large as those of reference beams.

According to Krassowska et al. [31], concrete beams reinforced with BFRP bars have shown the largest amount of cracks with greater widths, with the first perpendicular crack occurring when the load reached 10% of the ultimate load-carrying capacity of the sample. However, the flexural capacity of beams reinforced with FRP reinforcement has shown significant improvement. In terms of failure modes, observations made by Ashour AF [20] are significant. Additionally, it is important to note that the ACI Committee 440 [30] has highlighted the comparatively low transverse shear resistance exhibited by FRPs. Furthermore, Urbanski et al. [18] observed that beams reinforced with basalt bars displayed cracks that were three to four times wider than those observed in traditionally reinforced concrete beams. This underscores the necessity for further research aimed at developing a comprehensive model to accurately predict the shear capacity of FRP-reinforced concrete beams. Such efforts are crucial for advancing our understanding and ensuring the structural integrity of FRP-reinforced concrete beams.

This research endeavors to bridge this gap in the scientific discourse by embarking on a comprehensive comparative analysis. The study seeks to explore and contrast concrete beams that are reinforced with two prevalent types of FRP—namely, glass- and basalt fiber-reinforced polymer—against beams that are reinforced with traditional steel bars. Importantly, all specimens will be subjected to identical loading and environmental conditions, facilitating a nuanced examination of their performance under standardized parameters. Through this comparative approach, the research endeavors to yield a more holistic understanding of the inherent material properties of each type of reinforcement by identifying areas of strength and potential improvement across various reinforcement methodologies.

Furthermore, employing small-scale beam tests offers greater control over variables such as material properties and loading conditions, thereby enabling more precise comparisons between different reinforcement types.

This research empirically investigates small concrete beams that are reinforced with glass fiber-reinforced polymer (GFRP) bars, basalt fiber-reinforced polymer (BFRP) bars, and traditional steel reinforcement. The main objective is to analyze the performance of these materials within concrete beams, emphasizing strength, load-bearing capacity, failure modes, and deflection. Simultaneously, the research seeks to identify vulnerabilities in fiber-reinforced polymers (FRPs), laying the groundwork for future studies addressing these limitations and proposing improved reinforcement solutions for concrete beam structures.

2. Materials and Methods

2.1. Materials

The small beams were prepared using a concrete mixture containing CEM I 42.5R Portland cement. The cement content was set at 320 kg/m^3, with a water-to-cement ratio (w/c) of 0.5. The aggregate composition comprised 732 kg/m^3 of sand with a grain diameter of up to 2 mm and 1203 kg/m^3 of coarse natural aggregate with a grain diameter of up to 8 mm. To enhance the mixture, 3.2 kg/m^3 of superplasticizer was incorporated. For longitudinal reinforcement, 6 mm diameter S-500 steel bars with a tensile strength of 315 MPa, 6 mm diameter BFRPs with a tensile strength of 1180 MPa, and 8 mm diameter GFRPs with a tensile strength of 552 MPa were utilized, as depicted in Figure 1 below. The reinforcement design was made to resist the self-weight, with a safety factor of the concrete beam. The diameter variation between the two FRPs was used to achieve equivalent tensile strength and to counter the beam's own weight. This helped the investigation demonstrate the mechanical properties of the reinforcements under similar environmental conditions. All longitudinal reinforcements were prepared with a length of 940 mm.

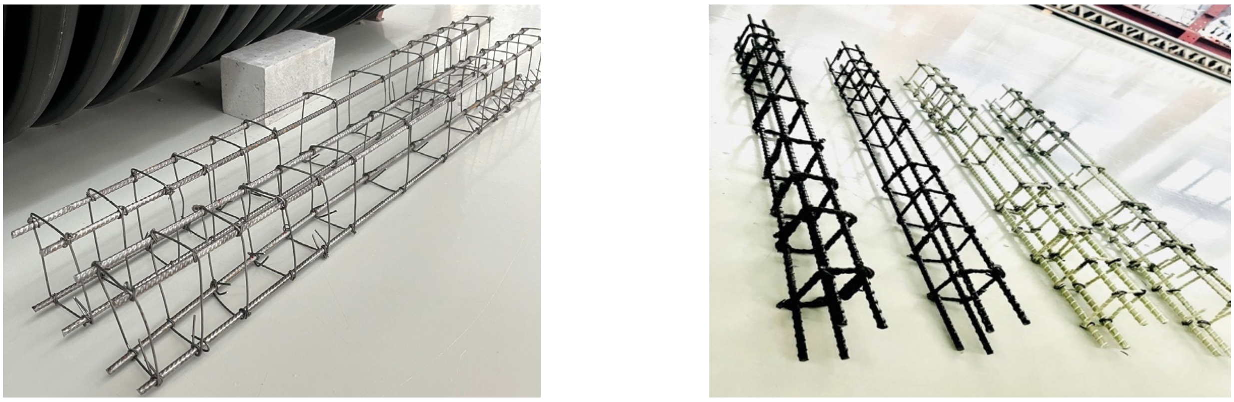

(a) (b)

Figure 1. Specimens' reinforcement setup: (**a**) steel reinforcement; (**b**) FRP reinforcement.

Before preparing the specimens, concrete strength tests were conducted to meet the required concrete standard based on strength. Three samples with a similar mix ratio were prepared for each strength test. Tests for the compressive strength of the concrete were executed following EN 12390-3:2009 [32], utilizing cubic samples with a side length of 100 mm. Tests for concrete tensile strength were carried out on samples measuring 100 × 100 × 400 mm, in accordance with EN 12390-5:2019 [33]. The modulus of elasticity was determined pursuant to EN 12390-13:2013 [34], using cylindrical specimens with a diameter of 160 mm and a height of 300 mm. The average test results were 59.66 MPa for compressive strength, 3.06 MPa for flexural strength, and 33.53 GPa for elastic modulus.

2.2. Description of Experimental Program

In order to enhance our comprehension of the performance of fiber-reinforced polymers in concrete beams, this research conducted an experimental program focusing on the ultimate load-bearing capacity; midspan deflection; average deformation at the top, middle, and bottom of concrete members under various load levels; and the failure modes of beams. The concrete specimens were mixed, cured, and tested in accordance with the EURO code. Six small beams measuring 80 × 120 × 1100 mm were employed in the study. These included two steel-reinforced beams (ABST-1 and ABST-2), two glass fiber-reinforced beams (ABGF-1 and ABGF-2), and two basalt fiber-reinforced beams (ABBF-1 and ABBF-2). The FRP-reinforced concrete beams were designed in accordance with the guidelines of ACI 440: 1R-06 standards [30]. The evaluation aimed to assess the mechanical characteristics and effectiveness of multiple reinforcing materials in enhancing the structural performance of concrete beams, as per the ACI 440.1R-06 standards [30]. All the beams were simply supported, with support points positioned 80 mm from the outer edge of the beams, resulting in span axes of 940 mm. Point loads are applied at 1/3 of the beam length on both sides. Throughout the test, the ultimate bending capacity of the element was determined, and various values were measured. These included deformations on the surface of the concrete member in the compressive, mid, and tensile zones, maximum deflection at midspan, and the development of cracks and failure modes of the beams. The beams underwent preloading with a 0 kN force. The force buildup occurred over 30 s per 2 kN, and the load was then held constant for approximately 30 s to record test readings. Subsequently, the force was incrementally increased by 2 kN until failure. The load application utilized a hydraulic cylinder, controlled from the control panel of the PZA machine. Deflection was gauged using inductive sensors from the Megatron-Munchen return spring, with specific locations designated for deflection measurements. Additionally, the progressive development of cracks and the shear capacity of the beams were meticulously recorded during the testing process. After each load phase until failure, every new crack was documented, and photographs were taken for the preparation of simulation drawings, as illustrated in Figure 2.

(**a**)

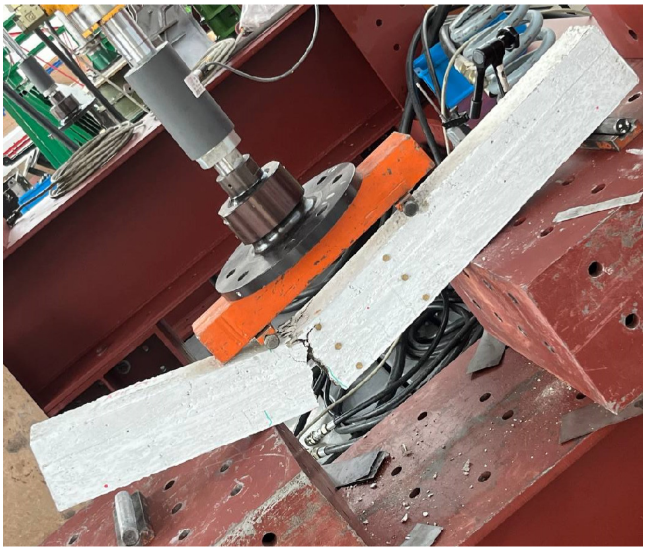

(**b**)

Figure 2. Sample specimen under initial and final loading states: (**a**) test sample under initial applied load; (**b**) test sample post ultimate load failure.

3. Test Results and Discussion

3.1. Ultimate Load-Bearing Capacity

The ultimate load is defined as the maximum load achieved by the beam. The loads being supported by concrete beams that were reinforced with GFRP bars markedly exceeded those reinforced with BFRP and steel bars. The concrete beams that were reinforced with BFRP showcased a superior load-bearing capacity compared to those that were reinforced with steel bars. Despite steel-reinforced concrete beams enduring more load before the onset of initial cracks, they ultimately failed sooner. BFRP-reinforced concrete beams manifested the early initiation of cracks when contrasted with steel-reinforced concrete beams but exhibited a higher ultimate load-bearing capacity, trailing only behind GFRP-reinforced concrete beams. The ultimate load-carrying capacity of the beam specimens before failure is depicted in Figure 3 below.

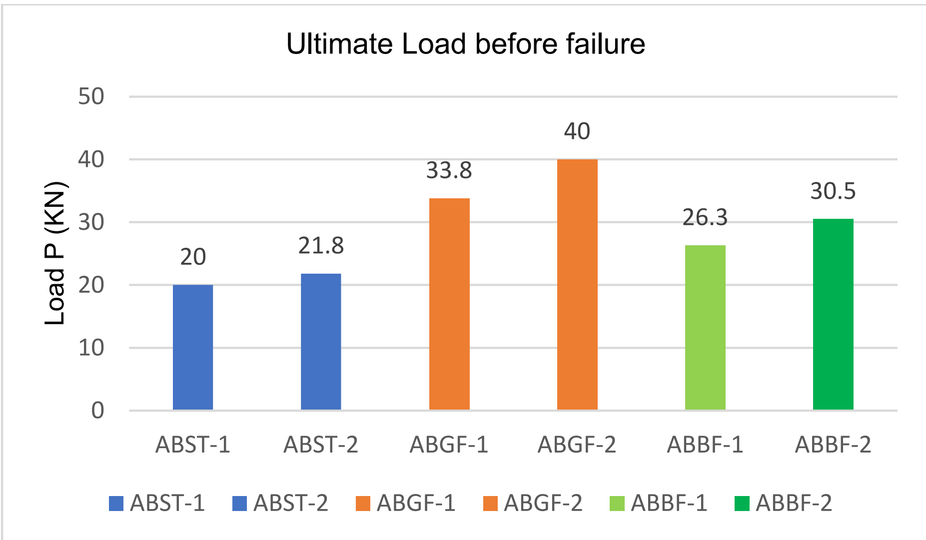

Figure 3. Ultimate load-bearing capacity of beam specimens.

Compared to concrete beams reinforced with steel bars, the average ultimate load-bearing capacity of the concrete beams reinforced with GFRP bars and BFRP bars increased by 76.5% and 35.8%, respectively. This increase can be attributed to the higher tensile strength of FRP bars compared to steel bars. One reason for the significant variation in the ultimate load-bearing capacity of beams reinforced with FRPs is the difference in the cross-sectional area of the reinforcements.

3.2. Deflection

The steel-reinforced concrete beams displayed similar behavior, experiencing failure at stresses of 20 kN and 21.8 kN, resulting in midspan deflections of 4.76 mm and 4.65 mm, respectively. Remarkably, the glass fiber-reinforced concrete beams exhibited remarkable strength, with ABGF-1 collapsing at 32 kN and ABGF-2 lasting until 40 kN. At the point of failure, midspan deflections measured 14.01 mm and 14.61 mm. The basalt fiber-reinforced concrete beams, performing between the steel- and GFRP-reinforced concrete beams, recorded failures at 26 kN (ABBF-1) and 30 kN (ABBF-2). The corresponding midspan deflections were 16.17 mm and 21.50 mm. Figure 4 illustrates the graphical implications of the maximum deflection observed in the sample specimens.

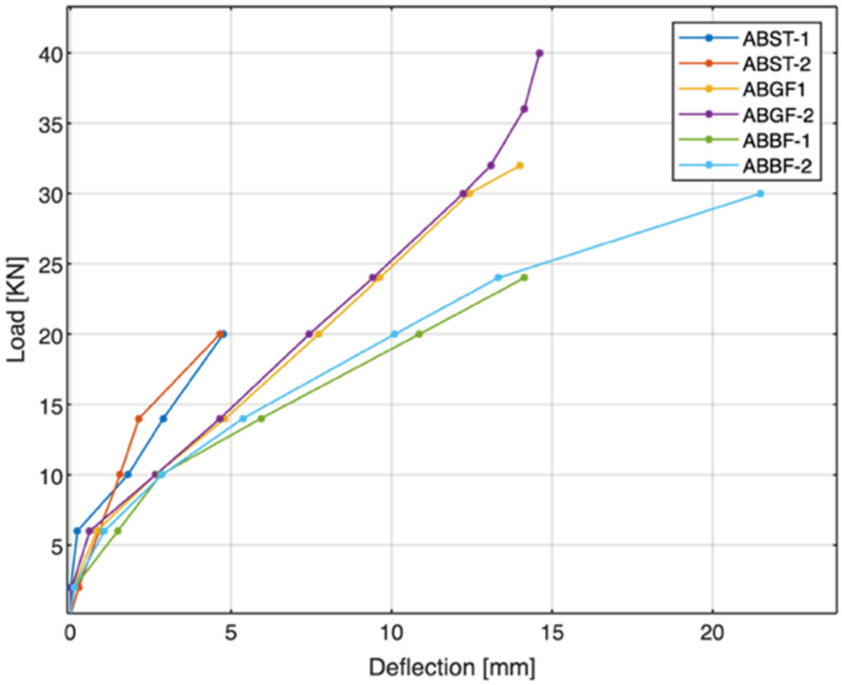

Figure 4. Load vs. deflection curves.

In this study, concrete beams that were reinforced with BFRP bars were found to exhibit higher deflection. Figure 5 illustrates the deflection of the beams under a regular load of 20 kN, where the GFRP-reinforced concrete beams displayed deflections of 7.73 mm (a 62% increase compared to the steel-reinforced beams) and 7.44 mm (a 60% increase compared to the steel-reinforced beams). On the other hand, the basalt fiber-reinforced beams demonstrated deflections of 10.87 mm (a 127% increase compared to the steel-reinforced beams and a 40% increase compared to the GFRP bar-reinforced concrete beams) and 10.10 mm (a 117% increase compared to the steel-reinforced concrete beams and a 35.75% increase compared to the GFRP-reinforced concrete beams). These findings underscore the greater flexibility of basal fiber-reinforced beams compared to glass fiber-reinforced beams.

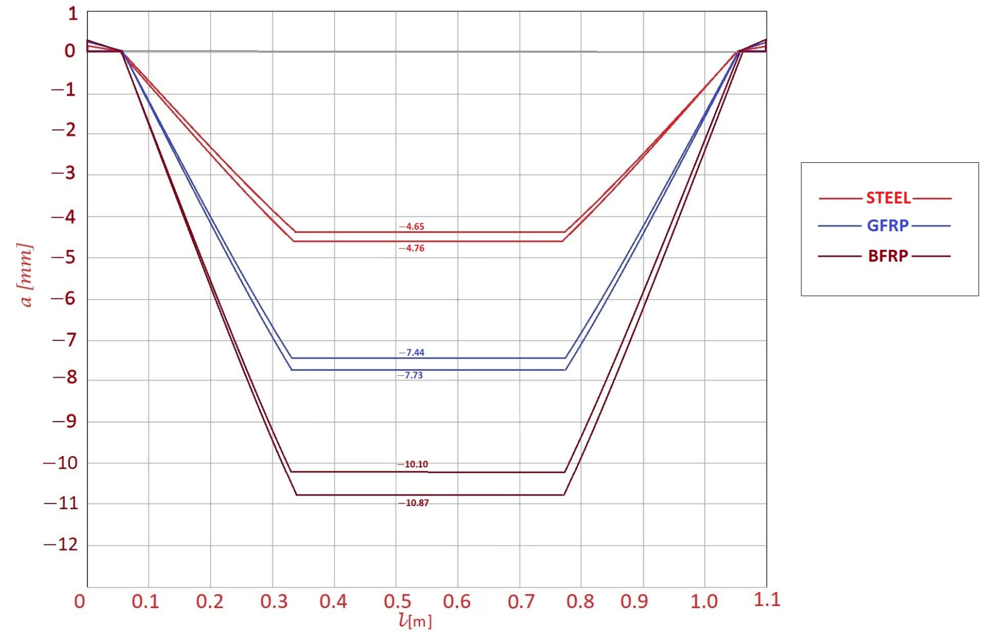

Figure 5. Deflection vs. position curves of beam specimens at 20 kN applied load (deflection data collected from gauges at the midpoint and both ends of the beams, measured at 2 kN load intervals).

3.3. Deformation of Concrete on the Surface of Different Sections of the Beam at Midspan

Figure 6 illustrates the deflection across different zones in the specimens. In Figure 6a, the compressive zone exhibited the least deformation: the steel-reinforced concrete beams measured 1.66 mm and 1.30 mm, the GFRP-reinforced concrete beams measured 1.45 mm and 2.73 mm, and the BFRP-reinforced beams measured 3.45 mm and 1.01 mm. In Figure 6c, the neutral zone demonstrated steel-reinforced concrete beams with 3.94 mm and 3.13 mm, GFRP-reinforced concrete beams with 3.77 mm and 4.38 mm, and BFRP-reinforced concrete beams with 6.86 mm and 7.95 mm. Figure 6c, representing the tensile zone, showed maximum deformation: the steel-reinforced concrete beams with 3.96 mm and 3.42 mm deformations, the GFRP-reinforced concrete beams with 7.04 mm and 9.05 mm, and the BFRP-reinforced concrete beams with 8.43 mm and 10.76 mm.

When comparing the values of concrete deformations at the same levels of beam loads, it was concluded that in the compressive zone, the highest deformations recorded in the case of concrete beams that were reinforced with BFRP and GFRP bars were 3.45‰ and 2.73‰, respectively. These values represented a 107.8% and 64.46% increase compared to the highest deformation recorded by the concrete beams that were reinforced with steel bars, which was 1.66‰. The most significant deformations in the compressive zone occurred in the case of concrete beams reinforced with GFRP bars.

In the mid-section of the beam, the highest deformation was recorded on concrete beams reinforced with BFRP, amounting to 7.95‰, which represented a 101.78% increase compared with the highest deformation recorded on concrete beams reinforced with steel bars, which was 3.94‰. Conversely, the highest deformation recorded for concrete beams reinforced with GFRP was 4.38‰, indicating an 11.17% increase from the deformation of concrete beams with steel reinforcement.

In the last section, which is the tensile zone, the highest deformation was observed for concrete beams that were reinforced with BFRP bars, measuring 10.76‰, and with GFRP bars, measuring 9.05‰. These values represented a 171.72% and 128.53% increase, respectively, compared to the highest deformation of concrete beams reinforced with steel bars, which was 3.96‰.

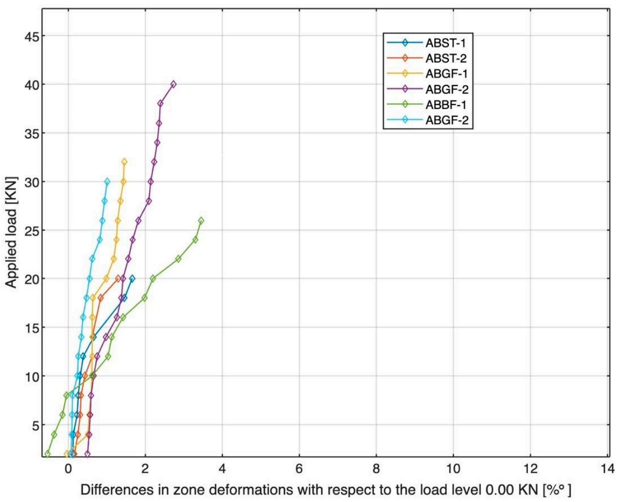

(**a**)

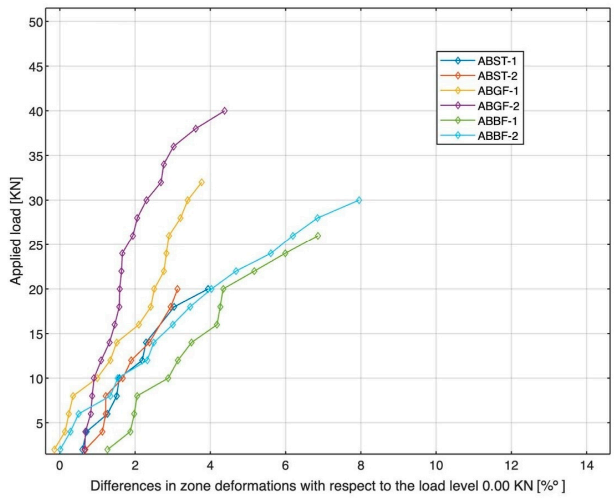

(**b**)

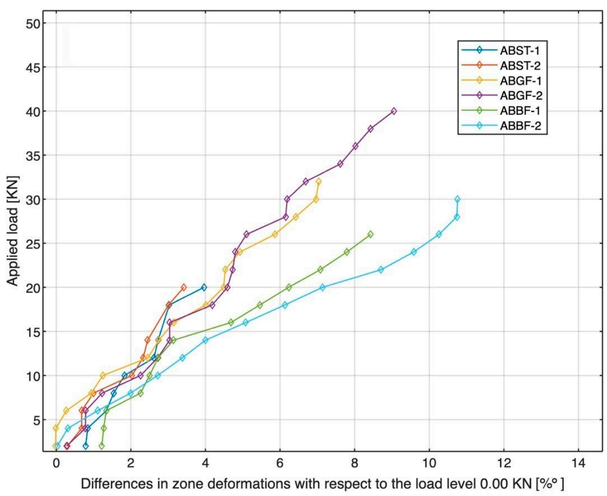

(**c**)

Figure 6. Deformation in different sections of beam specimens: (**a**) deformation in compressive zone; (**b**) deformation in mid-section; (**c**) deformation in tension zone.

3.4. Failure Modes

The analysis of various beam reinforcements unveiled a common pattern in the failure modes, providing valuable insights into their structural behavior under a load. Initially, cracks emerged in the flexural zone and midspan, accompanied by the development of additional vertical cracks within the shear span as the load intensified. Notably, steel-reinforced concrete beams exhibited midspan bending failure (Figure 7a,b), characterized by a premature failure.

In stark contrast, both the GFRP- and BFRP-reinforced concrete beams showcased ductile behavior, characterized by a gradual expansion of the cracks. Diagonal cracks were consistently observed in Figure 7c–f and were particularly notable in the GFRP- and BFRP-reinforced concrete beams, where they manifested as long diagonal cracks. The GFRP-reinforced concrete beams displayed significant deformations and wider crack widths compared to the steel-reinforced concrete beams. The BFRP-reinforced concrete beams exhibited a combination of diagonal tension and flexural failure modes.

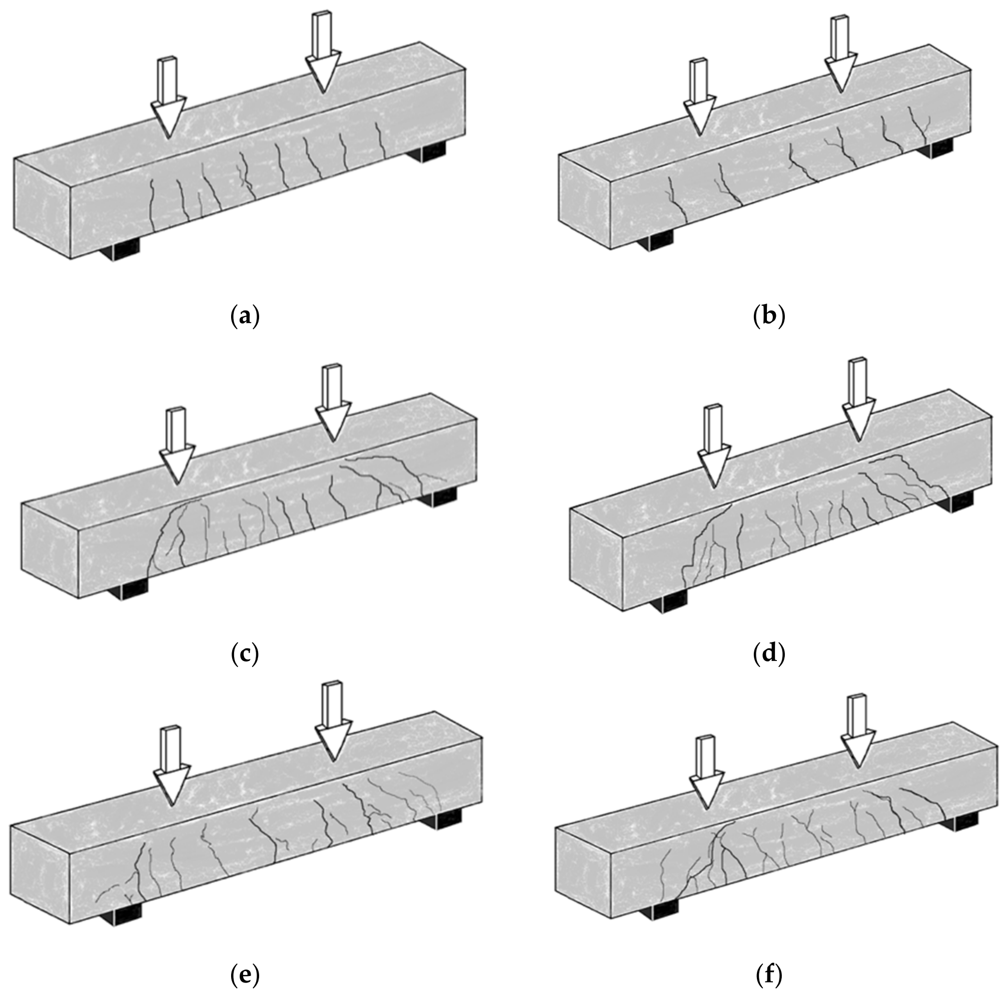

Figure 7. Crack development in tested concrete beams: (**a**) ABST-1; (**b**) ABST-2; (**c**) ABGF-1; (**d**) ABGF-2; (**e**) ABBF-1; (**f**) ABBF-2.

The failure modes exhibited distinct characteristics: the steel-reinforced concrete beams primarily failed due to flexural tension, while the GFRP-reinforced concrete beams demonstrated diagonal tension failure, subsequently leading to shear tension failure. The initiation of shear failure was marked by the emergence of a significant diagonal crack within the shear span, originating from the applied load. This crack propagated towards the point of GFRP reinforcement, eventually extending horizontally at the level of the GFRP bars towards the beam's support. Consequently, bond failure occurred between the longitudinal GFRP bars and the concrete, as illustrated in Figure 7. These detailed observations shed light on the intricate failure mechanisms that are inherent to different types of reinforced concrete beams.

In terms of failure modes, this study revealed a notable increase in crack formations within the FRP-reinforced concrete beams compared to their steel-reinforced counterparts. Specifically, beams reinforced with GFRP experienced shear failure, leading to longitudinal failure, with cracks propagating towards the support structures. The simulation images in Figure 7 provide a visual representation of the observed cracks in all the beam specimens before ultimate failure.

4. Conclusions

This research analyzes the critical shift from traditional steel reinforcement to the use of fiber-reinforced polymer (FRP) materials, specifically, glass fiber-reinforced polymer (GFRP) and basalt fiber-reinforced polymer (BFRP), in small concrete beams. Based on the experimental study, the following conclusions were drawn:

- A comprehensive investigation into the mechanical characteristics of GFRP- and BFRP-reinforced concrete beams in comparison to concrete beams that are reinforced with traditional steel bars was carried out.
- GFRP-reinforced concrete beams demonstrated an ultimate load-bearing capacity of 36.9 kN, outperforming BFRP-reinforced concrete beams and steel-reinforced concrete beams, which exhibited average ultimate load-bearing capacities of 28.4 kN and 20.9 kN, respectively.
- GFRP-reinforced concrete beams demonstrated notable strength and resilience, leading to later failure stages compared to their steel-reinforced counterparts.
- The deflection analysis highlighted the remarkable performance of GFRP-reinforced concrete beams, showcasing their superior strength and deformation properties in comparison to BFRP-reinforced concrete beams. However, both displayed higher deflections compared to concrete beams with steel reinforcement. On average, BFRP-reinforced concrete beams experienced a 122.85% increase in the maximum deflection, while GFRP-reinforced concrete beams exhibited a 61.21% increase when compared with steel-reinforced concrete beams.
- The examination of failure modes demonstrated that both GFRP- and BFRP-reinforced concrete beams exhibited a bending property before failure, while those that were reinforced with steel broke easily without bending much. This provides valuable insights into their distinct failure mechanisms.
- This study is limited to the examination of small concrete beams, which requires further studies regarding the applicability of the findings to full-sized beams. Additionally, further research and development of design models are recommended to address deflection issues associated with concrete beams reinforced by non-metallic reinforcements.

Author Contributions: Conceptualization: A.A.B., J.K. and M.K.-K.; Methodology and experiment: A.A.B., J.K. and M.K.-K.; Formal analysis and investigation: A.A.B.; Resources: A.A.B.; Writing—original draft preparation: A.A.B.; Writing—review and editing: J.K. and M.K.-K.; Supervision: J.K. and M.K.-K. All authors have read and agreed to the published version of the manuscript.

Funding: The research is funded from Bialystok University of Technology; Project number WI/WB-IIL/9/2023. This research work was financially supported by the National Centre for Research and Development, Poland; project number LIDER XIV Nr LIDER14/0206/2023.

Institutional Review Board Statement: Not applicable.

Informed Consent Statement: Not applicable.

Data Availability Statement: The original contributions presented in the study are included in the article, further inquiries can be directed to the corresponding author.

Conflicts of Interest: The authors declare no conflicts of interest.

References

1. Afroughsabet, V.; Biolzi, L.; Ozbakkaloglu, T. High-performance fiber-reinforced concrete: A review. *J. Mater. Sci.* **2016**, *51*, 6517–6551. [CrossRef]
2. Pros and Cons of Steel Reinforcement Bars, Mahadev Desai. Available online: https://gharpedia.com/blog/pros-and-cons-of-steel-reinforcement-bars/ (accessed on 11 November 2022).
3. PCA. *Types and Causes of Concrete Deterioration*; IS536; Portland Cement Association: Skokie, IL, USA, 2002.
4. Gkoumas, K.; Marques Dos Santos, F.L.; Van Balen, M.; Tsakalidis, A.; Ortega Hortelano, A.; Grosso, M.; Haq, G.; Pekár, F. *Research and Innovation in Bridge Maintenance, Inspection and Monitoring*; A European Perspective Based on Transport Research and Innovation Monitoring and Information System (TRIMIS), EUR 29650 EN; Publications Office of the European Union: Luxembourg, 2019; ISBN 978-92-79-99678-8. [CrossRef]
5. Solyom, S.; Di Benedetti, M.; Szijártó, A.; Balázs, G.L. Non-metallic reinforcements with different moduli of elasticity and surfaces for concrete structures. *Arch. Civ. Eng. Environ.* **2018**, *11*, 79–88. [CrossRef]
6. Rubino, F.; Nisticò, A.; Tucci, F.; Carlone, P. Marine Application of Fiber Reinforced Composites: A Review. *J. Mar. Sci. Eng.* **2020**, *8*, 26. [CrossRef]
7. Clyne, T.W.; Hull, D. *An Introduction to Composite Materials*, 3rd ed.; Cambridge University Press: Cambridge, UK, 2019; p. 345.

8. Hollaway, L.C. A review of the present and future utilisation of FRP composites in the civil infrastructure with reference to their important in-service properties. *Constr. Build. Mater.* **2010**, *24*, 2419–2445. [CrossRef]
9. Wang, Z.; Zhao, X.-L.; Xian, G.; Wu, G.; Raman, R.S.; Al-Saadi, S.; Haque, A. Long-term durability of basalt- and glass-fibre reinforced polymer (BFRP/GFRP) bars in seawater and sea sand concrete environment. *Constr. Build. Mater.* **2017**, *139*, 467–489. [CrossRef]
10. 5 Reasons to Use Fiber-Reinforced Polymer(FRP), Scott Reeve, 21 September 2022. Available online: https://www.creativecompositesgroup.com/blog/5-reasons-use-fiber-reinforced-polymer-frp (accessed on 6 May 2023).
11. Gudonis, E.; Timinskas, E.; Gribniak, V.; Kaklauskas, G.; Arnautov, A.K.; Tamulėnas, V. FRP reinforcement for concrete structures: State-of-the-art review of application and design. *Eng. Struct. Technol.* **2013**, *5*, 147–158. [CrossRef]
12. Ahmed, A.; Guo, S.; Zhang, Z.; Shi, C.; Zhu, D. A review on durability of fiber reinforced polymer (FRP) bars reinforced seawater sea sand concrete. *Constr. Build. Mater.* **2020**, *256*, 119484. [CrossRef]
13. Siddika, A.; Al Mamun, A.; Ferdous, W.; Alyousef, R. Performances, challenges and opportunities in strengthening reinforced concrete structures by using FRPs—A state-of-the-art review. *Eng. Fail. Anal.* **2020**, *111*, 104480. [CrossRef]
14. Adam, M.A.; Said, M.; Salah, A.; Elsheikh, A. Experimental and analytical study of high performance concrete beams reinforced with Basalt FRP bars. *Structures* **2023**, *55*, 510–530. [CrossRef]
15. Kudyakov, K.L.; Plevkov, V.S.; Nevskii, A.V. Strength and deformability of concrete beams reinforced by non-metallic fiber and composite rebar. *IOP Conf. Ser. Mater. Sci. Eng.* **2015**, *71*, 012030. [CrossRef]
16. Kosior-Kazberuk, M.; Krassowska, J. Analysis of deflection and cracking of concrete beams with non-metallic reinforcement. *Syst. Saf. Hum.-Tech. Facil.-Environ.* **2019**, *1*, 782–789. [CrossRef]
17. Elango, K.S.; Gopi, R.; Jayaguru, C.; Vivek, D.; Saravanakumar, R.; Rajeshkumar, V. Experimental investigation on concrete beams reinforced with basalt fiber reinforced polymer bars. *Mater. Today Proc.* **2021**, *45*, 2426–2429. [CrossRef]
18. Urbanski, M.; Lapko, A.; Garbacz, A. Investigation on concrete beams reinforced with basalt rebars as an effective alternative of conventional R/C structures. *Procedia Eng.* **2013**, *57*, 1183–1191. [CrossRef]
19. Krassowska, J.; Kosior-Kazberuk, M. The effect of steel and basalt fibers on the shear behavior of double-span fiber reinforced concrete beams. *Materials* **2021**, *14*, 6090. [CrossRef]
20. Ashour, A. Flexural and shear capacities of concrete beams reinforced with GFRP bars. *Constr. Build. Mater.* **2006**, *20*, 1005–1015. [CrossRef]
21. Kosior-Kazberuk, M.; Wasilczyk, R. Analiza ugięć i zarysowania betonowych belek ze zbrojeniem niemetalicznym. *Budownictwo Inżynieria Środowiska* **2017**, *8*, 172–183. Available online: https://pbc.biaman.pl/Content/54364/Budownictwo%20i%20In%C5%BCynieria%20%C5%9Arodowiska.%20Vol.8,%20no.4.pdf (accessed on 7 April 2024). (In Polish).
22. Sirimontree, S.; Keawsawasvong, S.; Thongchom, C. Flexural behavior, of concrete beam reinforced with GFRP bars compared to concrete beam reinforced with conventional steel reinforcements. *J. Appl. Sci. Eng.* **2021**, *24*, 883–890. [CrossRef]
23. Lebedev, M.P.; Startsev, O.V.; Kychkin, A.K. The effects of aggressive environments on the mechanical properties of basalt plastics. *Heliyon* **2020**, *6*, e03481. [CrossRef]
24. Ren, Y.; Wang, H.; Guan, Z.; Yang, K. Evaluation of the properties and applications of FRP bars and anchors: A review. *Rev. Adv. Mater. Sci.* **2023**, *62*, 20220287. [CrossRef]
25. Li, Y.; Yin, S.; Lu, Y.; Hu, C. Experimental investigation of the mechanical properties of BFRP bars in coral concrete under high temperature and humidity. *Constr. Build. Mater.* **2020**, *259*, 120591. [CrossRef]
26. Jin, Q.; Chen, P.; Gao, Y.; Du, A.; Liu, D.; Sun, L. Tensile strength and degradation of gfrp bars under combined effects of mechanical load and alkaline solution. *Materials* **2020**, *13*, 3533. [CrossRef] [PubMed]
27. Khan, Q.S.; Sheikh, M.N.; Hadi, M.N. Tension and compression testing of fibre reinforced polymer (FRP) bars. In Proceedings of the Joint Conference of the 12th International Symposium on Fiber Reinforced Polymers for Reinforced Concrete Structures (FRPRCS-12) & the 5th Asia-Pacific Conference on Fiber Reinforced Polymers in Structures (APFIS-2015), Nanjing, China, 14–16 December 2015; Wu, Z., Wu, G., Wang, X., Eds.; pp. 1–6. Available online: https://ro.uow.edu.au/eispapers/5008 (accessed on 7 April 2024).
28. Szmigiera, E.D.; Protchenko, K.; Urbański, M.; Garbacz, A. Mechanical properties of hybrid FRP bars and nano-hybrid FRP bars. *Arch. Civ. Eng.* **2019**, *65*, 97–110. [CrossRef]
29. Krassowska, J.; Wolka, P.; Protchenko, K.; Vidales-Barriguete, A. Testing the Influence of Metakaolinite and Zeolite on the Adhesion of BFRP and GFRP Bars to Concrete. *Materials* **2023**, *16*, 7435. [CrossRef] [PubMed]
30. *ACI 440.1R-06*; Guide for the Design and Construction of Concrete Reinforced with FRP Bars. ACI Committee 440. American Concrete Institute: Farmington Hills, MI, USA, 2006. Available online: https://www.concrete.org/Portals/0/Files/PDF/Previews/440_1R_15.pdf (accessed on 12 February 2024).
31. Krassowska, J.; Ramírez, C.P. Flexural Capacity of Concrete Beams with Basalt Fiber-Reinforced Polymer Bars and Stirrups. *Materials* **2022**, *15*, 8270. [CrossRef] [PubMed]
32. *EN 12390-3:2009*; Testing Hardened Concrete—Part 3: Compressive Strength of Test Specimens. European Committee for Standardization: Brussels, Belgium, 2009. Available online: https://i2.saiglobal.com/mpc2v/preview/497200114258.pdf?sku=855939_SAIG_NSAI_NSAI_2751255&nsai_sku=i-s-en-12390-3-2019-855939_saig_nsai_nsai_2751255 (accessed on 2 February 2024).

33. *EN 12390-5:2019*; Testing Hardened Concrete—Part 5: Flexural Strength of Test Specimens. European Committee for Standardization: Brussels, Belgium, 2019. Available online: https://cdn.standards.iteh.ai/samples/64401/9078b3193a544c26a16a278e66f0ae34/SIST-EN-12390-5-2019.pdf (accessed on 2 February 2024).
34. *EN 12390-13:2013*; Testing Hardened Concrete. Determination of Secant Modulus of Elasticity in Compression. European Committee for Standardization: Brussels, Belgium, 2013. Available online: https://knowledge.bsigroup.com/products/testing-hardened-concrete-determination-of-secant-modulus-of-elasticity-in-compression?version=standard (accessed on 2 February 2024).